Evaluation of Novel Third-Strand Bases for the Recognition of a C·G Base Pair in the Parallel DNA Triple-Helical Binding Motif

by **Isabelle Prévot** and **Christian J. Leumann***

Department of Chemistry and Biochemistry, University of Bern, Freiestrasse 3, CH-3012 Bern

We describe the synthesis and the incorporation into oligonucleotides of the novel nucleoside building blocks **9**, **10**, and **16**, carrying purine-like double H-bond-acceptor bases. These base-modified nucleosides were conceived to recognize selectively a cytosine·guanine (C·G) inversion site within a homopurine·homopyrimidine DNA duplex, when constituent of a DNA third strand designed to bind in the parallel binding motif. While building block **16** turned out to be incompatible with standard oligonucleotide-synthesis conditions, UV/triplex melting experiments with third-strand 15-mers containing β-D-nucleoside **6** (from **9**) showed that recognition of the four natural *Watson-Crick* base pairs follows the order G·C ≈ C·G > A·T > T·A. The recognition is sequence-context sensitive, and G·C or C·G recognition does not involve protonated species of β-D-nucleoside **6**. The data obtained fit (but do not prove) a structural model for C·G recognition *via* one conventional and one C–H···O H-bond. The unexpected G·C recognition is best explained by third-strand base intercalation. A comparison of the triplex binding properties of these new bases with those of 4-deoxothymine (5-methylpyrimidine-2(1*H*)-one, ^{4H}T), previously shown to be C·G selective but energetically weak, is also described.

Introduction. – Strong and sequence-specific triple-helix formation of oligonucleotides with genomic DNA can selectively interfere with gene expression on the level of transcription and, therefore, is of interest in medicinal chemistry and biotechnology [1][2]. Molecular recognition of a DNA duplex in the major groove *via* a third-strand oligonucleotide in either the parallel [3][4] or the antiparallel [5][6] binding motif, however, is restricted to homopurine – homopyrimidine DNA-sequence tracts. Despite considerable efforts over the past decade, a general recognition motif by third strands for any given DNA sequence is still elusive [7].

Approaches to overcome this sequence limitation in the past included the preparation and evaluation of new, unnatural bases that are designed to either target a pyrimidine base *via* one H-bond [8][9], or complete pyrimidine·purine base pairs [10][11]. The use of abasic sites or aromatic heterocycles that unselectively contribute to stacking without any base-reading capability *via* H-bonding was also evaluated, however, with limited success [12].

We recently reported on the selective recognition of G·C base pairs in DNA duplexes by parallel complementary oligodeoxynucleotides containing the unnatural nucleoside 7-(2′-deoxy-β-D-ribofuranosyl)hypoxanthine (^{7}H) [13]. Although only one H-bond between the bases ^{7}H and G can be formed, the ^{7}H·G·C base triple (*Fig. 1*) equals the stability of the canonical C^{+}·G·C base-triple (C = 2′-deoxy-5-methylcytidine) at pH 7.0. Empirically, we attributed the remarkable stability of the ^{7}H·G base pair to the assistance of two additional C–H···O H-bonds, flanking the conventional one (*Fig. 1*). As a consequence of this result, we explored whether the pyrimidine base

uracil can be recognized by ^{7}H in a similar way [14]. We were able to show that up to three uracil units within a 15 base-pair triplex target sequence (amounting to a 20% pyrimidine content) can be recognized, although with lower efficiency compared to a canonical triplex structure. We have since expanded on that theme and reported that selective recognition of a C·G base pair within the parallel DNA triple-helical binding motif can be achieved by a third strand containing the base 5-methylpyrimidin-2(1*H*)-one (^{4H}T) [15]. The third strand affinities (K_D) for a representative 15-mer duplex sequence containing all four *Watson-Crick* base pairs opposite to this base were C·G (26 nM) ≫ A·T (270 nM) ≈ T·A (350 nM) > G·C (*ca.* 700 nM).

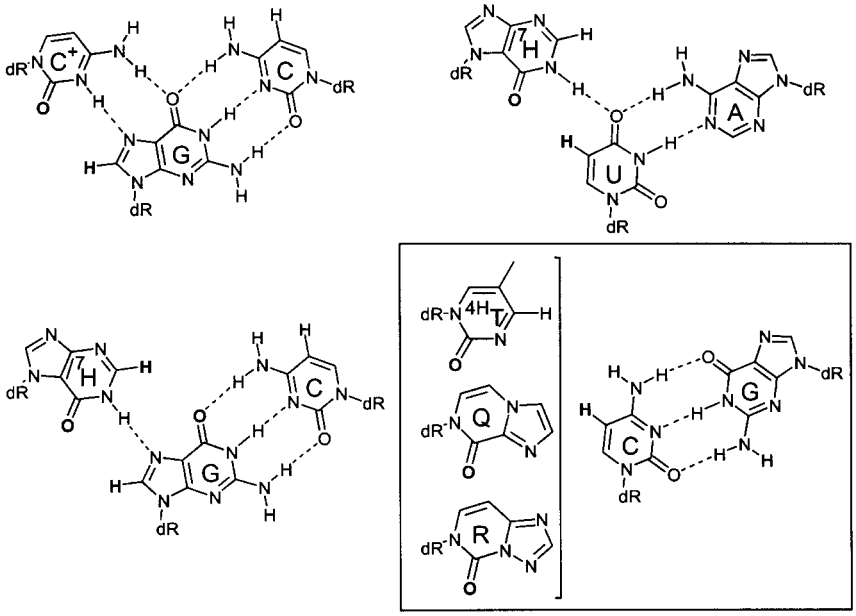

Fig. 1. *A selection of stable, known mono- and bidentate base triples in the parallel triple-helical binding motif, and the newly designed third-strand nucleosides ^{4H}T, Q, and R for the recognition of a C·G base pair* (box). Potential dipolar C–H···O interactions between spatially close arrangements of carbonyl O-atoms and sp^2 C–H bonds are highlighted in bold.

Along these lines, we report here on the synthesis and triple-helix-forming properties of the deoxynucleoside analogues Q (and R) with novel, purine-like heterocyclic bases (*Fig. 1*). The rationale behind the design was to increase third-strand affinity by increasing the stacking surface of the third-strand base while maintaining its double H-bond acceptor character that has been shown to confer C·G selectivity in the case of 5-methylpyrimidin-2(1*H*)-one (^{4H}T).

Results and Discussion. – *Synthesis of Nucleosides Q* (see **6**). Starting from the known 1*H*-imidazole-2-carboxamide (**1**) [16] (*Scheme 1*), base **3** was obtained in two

Scheme 1. *Synthesis of Nucleosides Q*

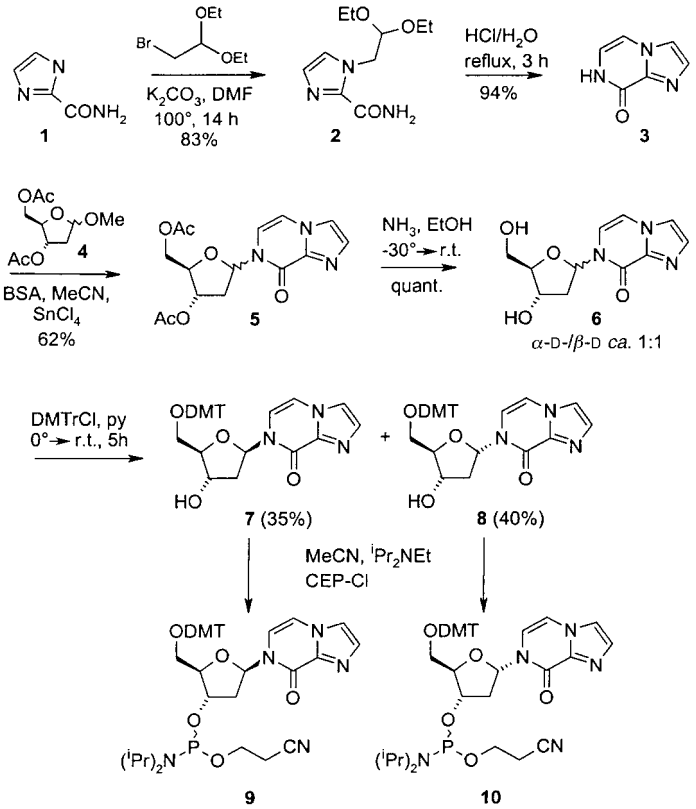

BSA = *N*,*O*-bis(trimethylsilyl)acetamide, CEP-Cl = 2-cyanoethyl diisopropylphosphoramidochloridite, DMTrCl = (4,4′-dimethoxytriphenyl)methyl chloride

steps by treatment of **1** with $BrCH_2CH(OEt)_2$, followed by acid hydrolysis of the acetal derivative **2** and condensation, in analogy to [17]. The base **3** in its silylated form was subsequently used for nucleoside formation according to the one-pot procedure of *Vorbrüggen* [18], in the presence of $SnCl_4$ as the *Lewis* acid promotor and **4** as the sugar component. The anomeric nucleoside-mixture **5** was thus obtained in 62% yield. As expected, no other nucleoside isomers could be isolated. Subsequently, the anomer mixture was saponified to give the unprotected nucleosides **6** (nucleosides Q) that were tritylated to yield the mixture **7**/**8**, which could be resolved by reversed-phase HPLC. Both anomers **7** and **8** were then converted separately to the corresponding phosphoramidite building blocks **9** and **10** for oligonucleotide synthesis. The configurational assignment (α-D,β-D) for **7** and **8** was made by comparison of the characteristic sugar-proton resonances in the ^{1}H-NMR spectra with those in the series of nucleosides R, for which independent proof of configuration was obtained by X-ray analysis (*vide infra*).

Synthesis of Nucleosides R (see **14**). The base triazolo[1,5-*c*]pyrimidin-5(3*H*)-one **12** (*Scheme 2*) that was needed for nucleoside synthesis[1]) was prepared in quantitative yield in one step from the known 3-aminocytosine hydrochloride (**11**) [20] by treatment with triethyl orthoformate and HCl. Nucleosidation was then effected again according to the *Vorbrüggen* procedure [18] with the anomers methyl 2-deoxy-3,5-di-*O*-acetyl-D-ribofuranoside (**4**) as the nucleosyl donor, the *in situ* persilylated base **12** as the acceptor, and $SnCl_4$ as the *Lewis* acid promotor, to give the anomeric-nucleoside mixture **13** in 82% yield. From the three potentially nucleophilic ring N-atoms of **12**, only that of the pyrimidine-ring moiety was found to be reactive under these conditions, which is in accord with the literature [19]. No other isomeric nucleosides could be isolated. Unfortunately, the anomer mixture could not easily be resolved at this stage, which prompted us to continue the synthesis with the mixture. Ammonolysis of the ester functions in **13** yielded the anomeric unprotected nucleosides **14** (nucleosides R) which, again, since they could not be efficiently separated, were directly converted to the trityl derivatives **15**. At this stage, the two anomeric forms could be separated by column chromatography. The β-D-anomer **15** was then further converted to phosphoramidite building block **16**.

Scheme 2. *Synthesis of Nucleosides R*

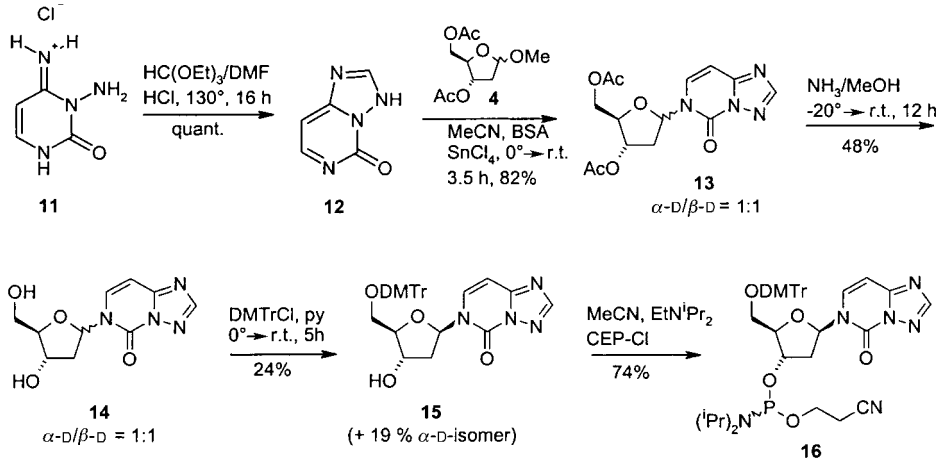

BSA = *N*,*O*-bis(trimethylsilyl)acetamide, DMTrCl = (4,4′-dimethoxytriphenyl)methyl chloride, CEP-Cl = 2-cyanoethyl diisopropylphosphoramidochloridite

To establish the point of attachment of the base and the configuration at the anomeric center, crystals of a chromatographically enriched α-D-fraction of **13** were obtained and subjected to X-ray analysis (*Fig. 2*)[2]). The crystal structure clearly

---

[1]) The synthesis of the β-D-ribonucleoside derivative of **12** and 2′,3′-dideoxy variants thereof has already been described [19].

[2]) Crystallographic data (excluding structure factors) for the structure reported in this paper have been deposited with the *Cambridge Crystallographic Data Centre* as deposition No. CCDC-169141. Copies of the data can be obtained, free of charge, on application to the CCDC, 12 Union Road, Cambridge CB2 1EZ UK (fax: +44(1223)336033; e-mail: deposit@ccdc.cam.ac.uk).

confirmed the structural assignments and showed, in addition, the glycosidic bond to be in the *anti* orientation. The sugar pucker is C(1′)-*exo*, arranging the base into a pseudoaxial position, a constellation that conforms well with the anomeric effect. The bond lengths and angles in the molecule are normal within experimental error.

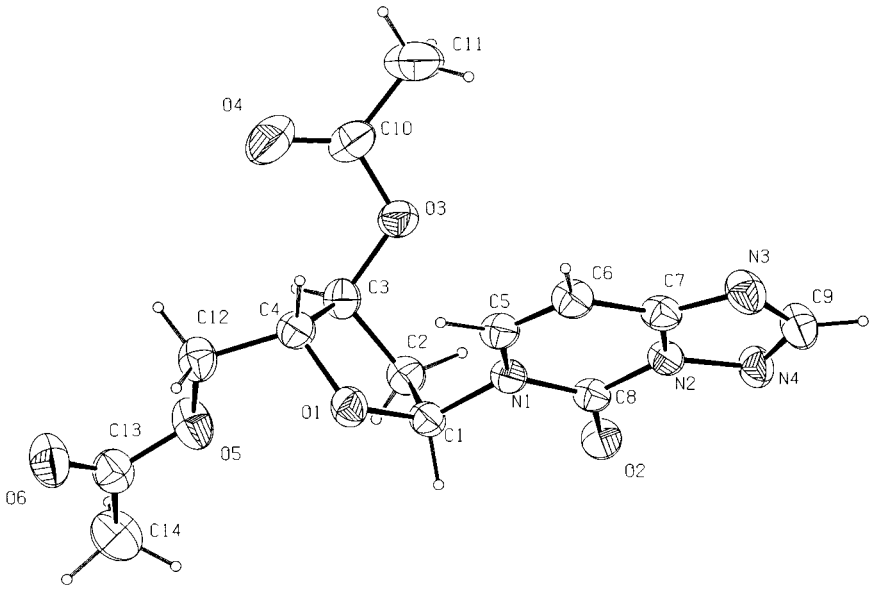

Fig. 2. *Perspective view of the* α-D-*anomer of* **13**. Thermal ellipsoids are drawn at the 50% probability level.

Synthesis of Oligonucleotides. Oligonucleotides were prepared by the well-established phosphoramidite protocol for automated DNA synthesis. The phosphoramidite building block **16** of the β-D-nucleoside R seemed to be incorporated into oligonucleotides with coupling yields of > 98% according to the trityl assay. It turned out, however, that after completed synthesis and deprotection, no full-length oligonucleotides could be detected by HPLC and ESI-MS. Instead, strand breakage occurred at the position of incorporation of **16**. Qualitative control experiments with **14** revealed that its nucleosidic bond is unstable under the detritylation conditions (2% CCl_3COOH in 1,2-dichloroethane) used during oligonucleotide assembly. Thus, it seems plausible that, after incorporation of **16**, acid-catalyzed depurination occurs, leading to an abasic site, at which strand cleavage *via* β-elimination occurs during ammonia treatment in the deprotection step.

Incorporation of building blocks **9** and **10** into oligonucleotides, on the other hand, proceeded smoothly. To analyze the base-pairing properties of ^{4H}T (the phosphoramidite building block of which was prepared as described [21]) and nucleosides Q towards double-stranded DNA, the oligonucleotide third strands and the DNA duplex targets depicted in the *Tables 1 – 4* were prepared. All oligonucleotides were purified by DEAE ion-exchange HPLC, their purity controlled by reversed-phase HPLC, and their structural integrity analyzed by ESI-mass spectrometry (see *Exper. Part*). *Fig. 3*

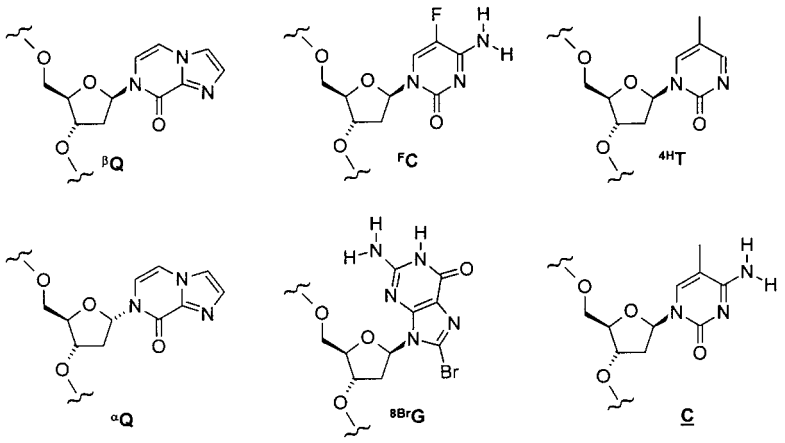

Fig. 3. *Formulae of nonconventional nucleosides and their corresponding symbols used in this study* (*cf. Tables 1–4*).

gives an overview of the chemical formulae and symbols used for the evaluation of triplex-binding properties, described in the following section.

Triplex-Forming Properties. First, insight into triplex stability and selectivity of ^{4H}T-containing third strands was obtained from UV/melting curves within the sequence context depicted in *Table 1*. Possible structures of base triples for all four natural target arrangements, as imposed by the parallel triple-helical binding motif, are depicted in *Fig. 4*. As noted earlier [15], there is a strong preference of $^{4H}T \cdot C \cdot G$ base-triple

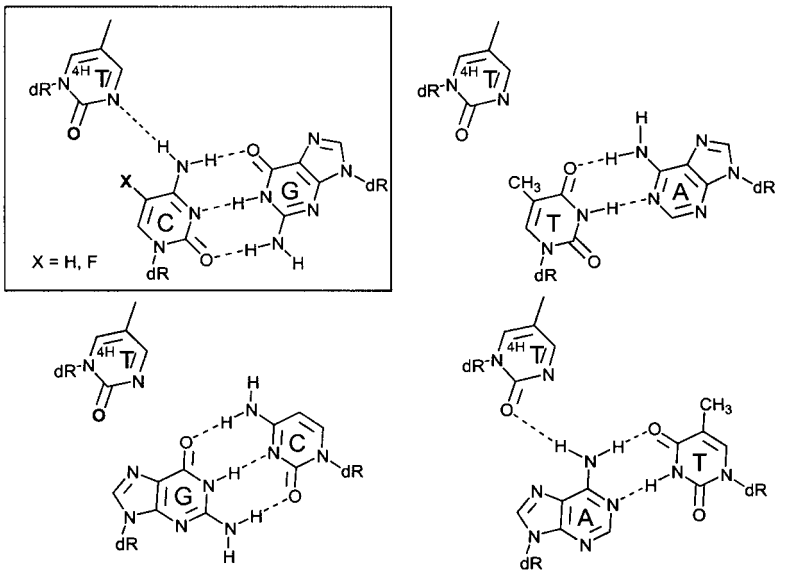

Fig. 4. *Visualization of base-triple arrangements resulting from sequence design* (*cf. Table 1*)

formation. The selectivity in target base-pair recognition follows the order C·G > G·C > A·T ≈ T·A over the whole pH range investigated. Differences in T_m between the ^{4H}T·G·C base-triple and the next best arrangement amount to 4.7–7.5 K, at all pH values. To probe the influence of the electrostatic environment at the interface of the target base cytosine and ^{4H}T, melting curves were measured with a duplex, in which the target deoxycytidine was replaced by 2′-deoxy-5-fluoro-cytidine (^{F}C, *Figs. 3* and *4*). As can bee seen from the corresponding T_m data (*Table 1*), this replacement strongly destabilizes the triple helix ($\Delta T_m = 8.3$ K, pH 6.0), underlining the importance of the local C–H bond for stability. So far, the results obtained are in accord with a structural model for C·G recognition (*Fig. 4*, top, left) relying on one conventional H-bond and, perhaps, an additional dipolar interaction between H–C(5) of cytosine and the carbonyl O-atom of ^{4H}T (*e.g.*, a C–H···O H-bond) weakly contributing to the stability of the base triple. Thus, a similar situation as found previously for a ^{7}H·U·A base triple within a parallel triple helix is encountered [14].

Table 1. T_m *Data* [°] *of Third-Strand Melting for the Indicated Triplexes.* For buffer conditions, see *Exper. Part.*

	Duplex target	5′-d(GCTAAAAAGA**X**AGAGAGATCG)-3′			
		3′-d(CGATTTTTCT**Y**TCTCTCTAGC)-5′			
	Third strand	5′-d(TTTTTC̲T**Z**TC̲TC̲TC̲T)-3′			
pH	**X**·**Y** (**Z** = ^{4H}T)				
	A·T	T·A	C·G	G·C	^{F}C·G
6.0	25.0	26.3	36.1	29.9	27.8
7.0	–[a])	10.8	18.3	8.4	14.2
8.0	–[a])	–[a])	7.0	–[a])	–[a])

[a]) No T_m detectable.

Experiments towards the determination of the quality of the novel ^{4H}T analogues $^{\alpha}$Q and $^{\beta}$Q (*Fig. 3*) in triple-helix formation were performed at first within the same sequence context as before (*Table 2*). The corresponding T_m data for melting of the $^{\alpha}$Q-containing triplex, not unexpectedly, showed drastically reduced thermal stabilities relative to the ^{4H}T-containing triplexes, irrespective of the nature of the target base-pair. With the exception of the G·C target, T_m data are reminiscent of a mismatch situation.

The picture becomes different when changing the anomeric configuration in Q. The $^{\beta}$Q-containing third strand, as expected, binds strongly to the C·G target with affinities that are similar to slightly inferior compared to ^{4H}T. Stability at pH 6.0 towards the duplex target base pairs decreases in the order C·G ≈ G·C > A·T > T·A. A surprising result is the binding of $^{\beta}$Q to the G·C target with similar thermal stability as to the C·G target. While C·G recognition may be related to an analogous structure as postulated for the case of ^{4H}T (*Fig. 5,a*), there is no obvious way for any H-bond formation between $^{\beta}$Q and G, due to the fact that both bases have only free H-bond acceptor sites (*Fig. 5,b*). A closer understanding of this fact clearly needed further experimental investigations.

Table 2. T_m *Data* [°] *of Third-Strand Melting for the Indicated Triplexes.* For buffer conditions, see *Exper. Part.*

Duplex target 5′-d(GCTAAAAAGA**X**AGAGAGATCG)-3′
3′-d(CGATTTTTCT**Y**TCTCTCTAGC)-5′
Third strand 5′-d(TTTTTCT**Z**TCTCTCT)-3′

pH	**X**·**Y** (**Z** = $^{\alpha}$Q)				**X**·**Y** (**Z** = $^{\beta}$Q)			
	A·T	T·A	C·G	G·C	A·T	T·A	C·G	G·C
6.0	18.0	21.0	22.8	28.1	26.3	19.9	33.0	34.0
6.5	10.2	12.7	–[a])	20.7	13.6	12.0	20.8	24.0
7.0	–[a])	–[a])	–[a])	19.4	4.7	–[a])16.1	13.0	
8.0	–[a])	–[a])	–[a])	–[a])	–[a])	–[a])	–[a])	–[a])

[a]) No T_m detectable.

To examine whether protonated species of $^{\beta}$Q might be involved in guanine recognition (*e.g.*, *Fig. 5*,*c*), we changed to the triple-helix sequence context shown in *Table 3*, in which all charged $C^+ \cdot G \cdot C$ base-triple arrangements were replaced by non-charged $T \cdot A \cdot T$ base triples. Thus, duplex recognition by third strands is intrisically pH insensitive in this case. As can be seen from *Table 3*, third-strand melting temperatures are virtually pH-independent in the pH range 6.0–8.0 for all duplex target base pairs, ruling out protonated species of $^{\beta}$Q to be involved in DNA binding near neutral pH. There may be a weak dependence due to partial protonation of $^{\beta}$Q, in the case of $A \cdot T$ base-pair recognition, which shows a tendency to increased triplex stability at decreased pH. The relative order of stability of $^{\beta}$Q follows the line $G \cdot C > A \cdot T > C \cdot G \approx T \cdot A$. Thus, the preferences are quite different compared to that of the previous system (*Table 2*), indicating a strong sequence dependence in the recognition preferences of $^{\beta}$Q.

At this point, the question arose whether noncanonical duplex base pairs might be involved in base-triple formation with $^{\beta}$Q. One such noncanonical arrangement could arise from a conformational shift of the base from the *anti*- to the *syn*-form of the target deoxyguanosine residue upon complexation with $^{\beta}$Q (*Fig. 5*,*d*). Admitting protonation of the *Watson-Crick* partner cytosine, the thermodynamic driving force could be the formation of a total of four instead of only three H-bonds in this base triple. It was found earlier that guanosine mononucleotides prefer the *syn*-conformation of the base [22]. Furthermore, deoxyguanosine residues with the base in the *syn*-conformation are

Table 3. T_m *Data* [°] *of Third-Strand Melting for the Indicated Triplexes.* For buffer conditions, see *Exper. Part.*

Duplex target 5′-d(GCTAAAAAAA**X**AAAAAAATCG)-3′
3′-d(CGATTTTTTTT**Y**TTTTTTTTAGC)-5′
Third strand 5′-d(TTTTTTTT**Z**TTTTTTT)-3′

pH	**X**·**Y** (**Z** = $^{\beta}$Q)			
	A·T	T·A	C·G	G·C
6.0	27.0	21.0	23.1	32.7
6.5	26.3	22.1	22.0	32.7
7.0	25.6	22.6	22.2	33.3
8.0	25.4	22.8	22.9	33.3

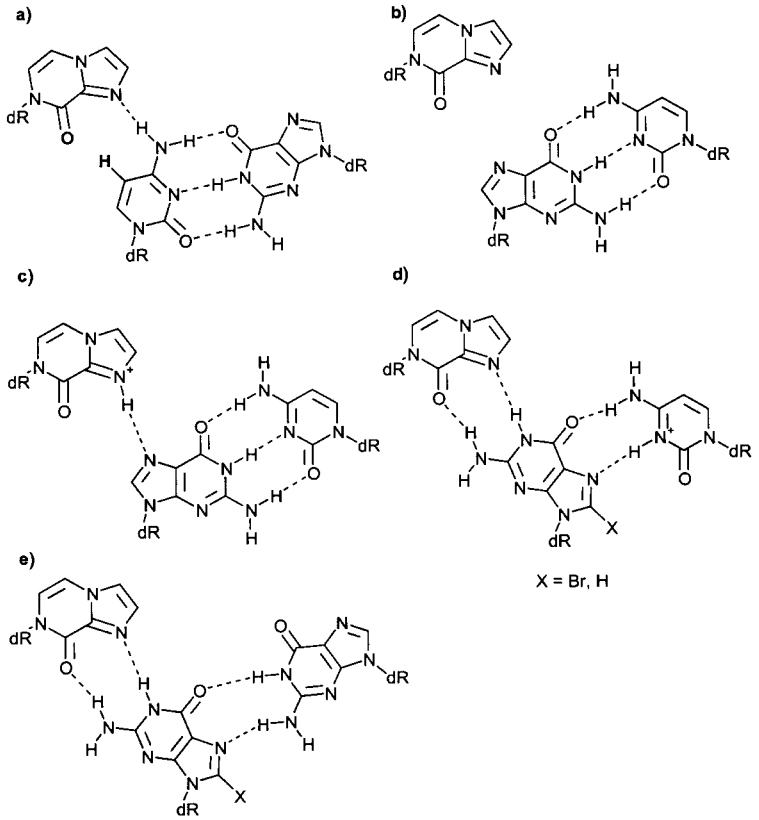

Fig. 5. *Visualization of selected, putative base-triple arrangements in the triplexes described in* Tables 2–4

encountered, *e.g.*, in left-handed Z-DNA duplexes [22], or in duplexes containing G · A [23] or G · G [24] mismatches. Introduction of bulky groups as, *e.g.*, a Br-atom at C(8) of guanine are known to enforce the *syn*-conformation of the base in the respective nucleoside unit [22].

A test whether such noncanonical base triples (*Fig. 5*,*d* and *e*) might be created by a $^{\beta}$Q residue in the third strand was performed in the sequence context described in *Table 4*. Forcing the target base G into a *syn*-conformation, either by means of its 8-bromo derivative ^{8Br}G against C or G, or simply by creating a G · G mismatch situation in the target duplex, did lead to increases in thermal stability of only 2.9–3.2 K, relative to the canonical G · C base pair, at the best. It thus seems unlikely that such non-canonical base triples were formed.

Conclusions. – The results obtained in this study clearly show that, inspite of increasing the stacking surface in $^{\beta}$Q relative to ^{4H}T, no gain in affinity to a C · G target is observed within the parallel triple-helical binding motif. To the contrary, a loss of selectivity was encountered. Various factors could be responsible for this. For example, the geometry of the H-bond acceptor sites in $^{\beta}$Q is not identical to that of ^{4H}T, which

Table 4. T_m *Data* [°] *of Third-Strand Melting for the Indicated Triplexes* (duplex T_m's in parenthesis). For buffer conditions, see *Exper. Part.*

Duplex target 5′-d(GCTAAAAAGA**X**AGAGAGATCG)-3′
3′-d(CGATTTTTCT**Y**TCTCTCTAGC)-5′
Third strand 5′-d(TTTTTCT**Z**TCTCTCT)-3′

X · **Y** (**Z** = $^{\beta}$Q)	pH 6.0	pH 7.0	pH 8.0
^{8Br}G · G	37.2 (53.1)	18.8 (53.3)	–[a]) (51.9)
G · G	36.9 (50.0)	18.0 (52.2)	–[a]) (49.9)
^{8Br}G · C	31.0 (55.0)	15.0 (55.2)	–[a]) (55.1)
G · C	34.0 (59.0)	13.0 (59.0)	–[a]) (59.0)

[a]) No T_m detectable.

might result in backbone distorsion upon base-pair formation with a C · G target. Alternatively it can not be excluded that other modes of recognition as, *e.g.*, selective intercalation of $^{\beta}$Q in between target duplex base pairs does occur. In fact, the affinity of $^{\beta}$Q for the G · C base-pair may be the result of such an interaction.

It also remains open at this point whether the alignment of the carbonyl group of ^{4H}T with the H–C(5) of its target base cytosine structurally occurs; and if so, whether this arrangement contributes to the stability of the base triple, or has just to be considered as a neutral *Van der Waals* contact. To determine this, more structural and biophysical work as, *e.g.*, an IR-spectroscopic investigation, is necessary.

Investigation of the pairing properties of ^{4H}T in the DNA triple-helix context teached us that base · base recognition relying on one H-bond only can be highly selective. The major problem to be overcome in such cases, however, is the low target affinity. Again in the context of DNA triplexes, it might, therefore, be of interest to combine bases that recognize pyrimidines selectively by one H-bond, like ^{4H}T, with sugar-backbone modifications that are known to enhance DNA affinity in a non-base-dependent manner, *e.g.*, *via* conformational restriction, as in locked nucleic acid (LNA) [25][26] or *via* phosphate-charge screening, as in the case of 2′-aminoethyl-modified RNA [27][28]. First attempts to use LNA in combination with such bases for targeting pyrimidines in triple-helix formation are encouraging [29].

Financial support from the *Swiss National Science Foundation* (*C.J.L.*) and the *Roche Research Foundation* (*I.P.*) is gratefully acknowledged. We thank the BENEFRI Small Molecule Crystallography Service directed by Prof. *Helen Stoeckli-Evans* for measuring the X-ray structure.

Experimental Part

General. Solvents for chromatography and extractions: technical grade, distilled; Reagents: highest grade available from *Fluka* or *Aldrich*. Standard conventions and equipment were used for analysis and characterization of new compounds (^{1}H- and ^{13}C-NMR: δ in ppm, J in Hz. ^{31}P-NMR (202 MHz); δ in ppm relative to PPh_3 as external standard).

*1-(2,2-Diethoxyethyl)-1*H*-imidazole-2-carboxamide* (**2**). Amide **1** (2.0 g, 18 mmol; prepared as described [17]) was dissolved in dry DMF (50 ml). After addition of K_2CO_3 (6 g, 41 mmol) and $BrCH_2CH(OEt)_2$ (3 ml, 18 mmol), the soln. was heated to 100° overnight. After filtration, the residual solid was washed with DMF (50 ml) and the filtrate evaporated. CC (SiO_2, AcOEt → AcOEt/MeOH 9:1) yielded **2** (3.39 g, 83%). White solid. ^{1}H-NMR (300 MHz, $CDCl_3$): 7.22 (br. *s*, 1 H); 7.10 (*s*, 1 H); 6.99 (*s*, 1 H); 5.40 (br. *s*, 1 H); 4.68 (*t*, J = 5.49, 1 H); 4.51 (*d*, J = 5.16, 2 H); 3.69 (*m*, 2 H); 3.46 (*m*, 2 H); 1.14 (*t*, J = 6.99, 6 H). ^{13}C-NMR (300 MHz, $CDCl_3$):

137.76, 127.42, 126.56, 101.74, 63.91, 50.98, 15.12. HR-LSI-MS: 228.134817 ($[M+H]^+$, $C_{10}H_{18}N_3O_3^+$; calc. 228.134540).

*Imidazo[1,2-*a*]pyrazin-8(7*H*)-one* (**3**). To a suspension of **2** (3.40 g, 25 mmol) in H_2O (68 ml), 5% HCl soln. (17 ml) was added. After refluxing for 3 h, the solvents were evaporated. The resulting product was recrystallized from MeOH: **3** (1.90 g, 94%). White needles. ^{1}H-NMR (300 MHz, (D_6)DMSO): 12.21 (br. *s*, 1 H); 8.16 (*d*, *J* = 1.47, 1 H); 7.99 (*d*, *J* = 1.47, 1 H); 7.72 (*d*, *J* = 5.52, 1 H); 7.22 (*dd*, *J* = 5.88, 5.52, 1 H). ^{13}C-NMR (300 MHz, (D_6)DMSO): 126.08, 120.33, 118.75, 107.56. HR-LSI-MS: 135.043262 ($[M+H]^+$, $C_6H_5N_3O^+$; calc. 135.043010).

*7-(3′,5′-Di-*O*-acetyl-2′-deoxy-*D*-ribofuranosyl)imidazo[1,2-*a*]pyrazin-8(7*H*)-one* (**5**). To a suspension of **3** (1.8 g, 13.3 mmol) in MeCN (150 ml), **4** (3.0 g, 13 mmol) and BSA (10.8 ml, 44 mmol) were added, and the mixture was stirred at r.t. for 30 min. After cooling to 0°, $SnCl_4$ (5.5 ml, 52 mmol) was added and the ice bath removed. Standard aq. workup after 3.5 h, followed by CC (SiO_2, AcOEt/MeOH 9:1) gave **5** (α-D/β-D 1:1; 2.70 g, 62%). Yellowish oil. ^{1}H-NMR (300 MHz, $CDCl_3$): 7.47 (*d*, *J* = 1.11, 2 H); 7.36 (*d*, *J* = 1.1, 2 H); 7.18 (*dd*, *J* = 6.24, 4.05, 2 H); 6.94 (*d*, *J* = 6.24, 2 H); 6.61 (*dd*, *J* = 8.46, 5.52, 1 H); 6.49 (*dd*, *J* = 6.99, 2.22, 1 H); 5.18 (*m*, 2 H); 4.59 (*m*, 1 H); 4.31 (*dd*, *J* = 4.41, 2.94, 2 H); 4.24 (*m*, 2 H); 4.16 (*dd*, *J* = 4.41, 3.69, 1 H); 2.84 (*m*, 1 H); 2.54 (*m*, 1 H); 2.25 (*m*, 1 H); 2.10 (*m*, 1 H); 2.06, 2.05, 1.97, 1.92 (4*s*, 12 H). ^{13}C-NMR (300 MHz, $CDCl_3$): 170.20, 170.09, 169.80, 152.85, 152.78, 137.01, 136.77, 133.19, 133.11, 116.59, 116.36, 114.37, 113.80, 107.43, 106.45, 86.44, 84.26, 84.04, 81.99, 74.14, 74.09, 63.66, 63.56, 38.45, 37.59, 20.65, 20.63, 20.55, 20.53. HR-LSI-MS: 336.119420 ($[M+H]^+$, $C_{15}H_{18}N_3O_6^+$; calc. 336.119561).

*7-(2′-Deoxy-*D*-ribofuranosyl)imidazo[1,2-*a*]pyrazin-8(7*H*)-one* (**6**). To a soln. of **5** (650 mg, 1.9 mmol) in EtOH (100 ml), conc. NH_3 soln. (100 ml) was added at −30°. The soln. was allowed to reach r.t. overnight. Evaporation yielded **6** (486 mg, 100%). Beige solid. ^{1}H-NMR (300 MHz, (D_6)DMSO): 8.43 (br. *s*, 0.5 H); 7.80 (*s*, 2 H); 7.60 (*t*, *J* = 2.94, 2 H); 7.48 (*d*, *J* = 2.94, 2 H); 7.37 (*m*, 2 H); 6.50 (*dd*, *J* = 6.98, 6.62, 1 H); 6.43 (*dd*, *J* = 7.72, 2.94, 1 H); 4.28 (br. *m*, 2 H); 4.26 (br. *t*, 2 H); 3.83 (*m*, 2 H); 3.61 (*m*, 2 H); 3.43 (*d*, *J* = 4.78, 2 H); 2.66 (*m*, 1 H); 2.11 (*m*, 3 H). ^{13}C-NMR (300 MHz, (D_6)DMSO): 171.99, 133.04, 124.70, 117.88, 116.18, 115.26, 107.95, 107.34, 91.34, 89.53, 87.79, 85.17, 83.52, 70.86, 62.04, 61.65, 22.71. HR-LSI-MS: 252.098770 ($[M+H]^+$, $C_{11}H_{14}N_3O_4^+$; calc. 252.098431).

*7-{2′-Deoxy-5′-*O*-[(4,4′-dimethoxytriphenyl)methyl]-*D*-ribofuranosyl}imidazo[1,2-*a*]pyrazin-8(7*H*)-one* (**7**/**8**). To a soln. of **6** (400 mg, 1.6 mmol) in pyridine (5 ml) at 0°, DMTrCl (600 mg, 1.7 mmol) was added in 6 portions. After stirring for 2 h at r.t., the reaction was quenched with MeOH (1 ml), the mixture evaporated, and the residue purified by CC (SiO_2, CH_2Cl_2/MeOH/Et_3N 97:2:1): **7**/**8** (0.715 g, 80%). The mixture **7**/**8** was separated by reversed-phase HPLC (gradient MeCN (1% Et_3N/H_2O).

*β-*D*-Anomer* **7**: 320 mg (35%). White solid. ^{1}H-NMR (300 MHz, $CDCl_3$): 7.49 (*d*, *J* = 1.11, 1 H); 7.39 (*m*, 3 H); 7.28 (*m*, 9 H); 6.82 (*d*, *J* = 9.18, 4 H); 6.76 (*d*, *J* = 5.88, 1 H); 6.70 (*t*, *J* = 6.70, 1 H); 4.64 (*m*, 1 H); 4.11 (*dd*, *J* = 7.35, 3.30, 1 H); 3.77 (*s*, 6 H); 3.48 (2*dd*, *J* = 10.65, 10.29, 3.30, 2.94, 2 H); 2.60 (*m*, 1 H); 2.28 (*m*, 1 H). ^{13}C-NMR (300 MHz, $CDCl_3$): 138.12, 130.28, 130.08, 130.00, 128.22, 128.07, 127.93, 127.74, 126.90, 126.61, 116.53, 115.81, 113.23, 113.02, 108.18, 105.96, 88.73, 88.04, 86.02, 82.53, 77.21, 55.24, 41.52. LSI-MS: 554 (14, M^+). HR-LSI-MS: 554.229250 ($[M+H]^+$, $C_{32}H_{32}N_3O_6^+$; calc. 554.229111).

*α-*D*-Anomer* **8**: 360 mg (40%). ^{1}H-NMR (300 MHz, $CDCl_3$): 7.43 (*d*, *J* = 6.99, 3 H); 7.27 (*m*, 10 H); 7.04 (*d*, *J* = 5.88, 1 H); 6.85 (*d*, *J* = 8.82, 4 H); 6.48 (*dd*, *J* = 7.35, 1.83, 1 H); 4.53 (*m*, 1 H); 3.80 (*s*, 6 H); 3.22 (*dd*, *J* = 5.13, 4.80, 2 H); 2.87 (*m*, 1 H); 2.45 (*d*, *J* = 14.7, 1 H). ^{13}C-NMR (300 MHz, $CDCl_3$): 158.5, 144.59, 135.798, 135.70, 132.91, 130.14, 130.12, 130.06, 130.0, 129.11, 128.22, 128.09, 127.92, 127.89, 127.81, 127.75, 127.04, 126.87, 116.59, 115.96, 113.16, 113.01, 106.03, 88.87, 87.94, 86.46, 84.29, 72.68, 71.57, 64.20, 55.22, 41.49. FAB-MS (pos.): 554 (13, M^+). HR-LSI-MS: 554.227480 ($[M+H]^+$, $C_{32}H_{32}N_3O_6^+$; calc. 554.229111).

*7-{2′-Deoxy-5′-*O*-[(4,4′-dimethoxytriphenyl)methyl]-β-*D*-ribofuranosyl}imidazo[1,2-*a*]pyrazin-8(7*H*)-one 3′-(2-Cyanoethyl Diisopropylphosphoramidite)* (**9**). At r.t., 2-cyanoethyl diisopropylphosphoramidochloridite (74 µl, 0.34 mmol) was added dropwise to a soln. of **7** (140 mg, 0.25 mmol) and ^{i}Pr$_2$NEt (110 µl, 0.66 mmol) in THF (5 ml) at r.t. After 2 h at r.t., the reaction was quenched with sat. $NaHCO_3$ soln. and the mixture extracted with CH_2Cl_2 (2×). After drying ($MgSO_4$) and evaporation of the org. phase, the residue was purified by CC (SiO_2, 10% Et_3N in AcOEt/hexane 1:1): **9** (80%; 1:1 diastereoisomer mixture). White foam. ^{1}H-NMR (300 MHz, $CDCl_3$): 7.50–7.20 (*m*, 43 H); 7.15 (*d*, *J* = 3.63, 2 H); 7.10 (*d*, *J* = 3.57, 1 H); 6.85 (*d* + *m*, *J* = 5.34, 13 H); 6.70 (*dd*, *J* = 7.44, 1.14, 2 H); 6.56 (*dd*, *J* = 3.18, 1.38, 1 H); 4.85 (*m*, 2 H); 4.73 (*dd*, *J* = 2.37, 2.52, 1 H); 4.55 (*dd*, *J* = 2.28, 2.52, 1 H); 4.51 (*d*, *J* = 3.54, 1 H); 4.05 (*m*, 1 H); 3.87 (*t*, *J* = 3.78, 3 H); 3.81 (*s* + *m*, 20 H); 3.26 (*m*, 8 H); 3.18 (*m*, 2 H); 2.90 (*m*, 3 H); 2.60 (*t*, *J* = 3.78, 3 H); 2.36 (*m*, 3 H); 1.10–1.35 (*m*, 26 H). ^{13}C-NMR (300 MHz, $CDCl_3$): 156.34, 151.02, 142.42, 142.35, 135.26, 133.60, 133.52, 133.44, 131.23, 131.03, 130.98, 127.84, 127.82, 125.92, 125.91, 125.87, 125.83, 125.79, 125.69, 124.83, 124.78, 124.67, 114.40, 113.91, 113.86, 111.13, 111.11,

111.02, 104.25, 104.03, 86.51, 85.64, 85.57, 85.34, 84.81, 84.49, 84.35, 84.26, 75.26, 75.04, 74.84, 74.42, 72.15, 72.10, 70.41, 62.07, 61.89, 56.39, 56.35, 55.47, 53.03, 44.38, 43.29, 39.36, 38.63, 38.59, 19.76, 19.27, 16.81, 16.77, 6.37. ^{31}P-NMR (202 MHz, $CDCl_3$): 140.1, 139.7. HR-LSI-MS: 770.332580 ($[M+H]^+$, $C_{41}H_{49}N_5O_8P^+$; calc. 770.331878).

*7-[2′-Deoxy-5′-*O*-[(4,4′-dimethoxytriphenyl)methyl]-α-*D*-ribofuranosyl]imidazo[1,2-*a*]pyrazin-8(7*H*)-one 3′-(2-Cyanoethyl Diisopropylphosphoramidite* (**10**). As described for **9**, from **8** (140 mg, 0.25 mmol): **10** (207 mg, 79%). Colorless foam. ^{1}H-NMR (300 MHz, $CDCl_3$): 7.20–7.60 (*m*, 15 H); 6.60–6.90 (*m*, 3 H); 4.70 (*m*, 1 H); 3.78 (*s*, 3 H); 3.70 (*m*, 1 H); 3.75 (*s*, 3 H); 3.54 (*m*, 2 H); 2.2–2.8 (*m*, 4 H); 1.0–1.5 (*m*, 16 H). ^{13}C-NMR (300 MHz, $CDCl_3$): 156.6, 156.59, 156.50, 156.47, 150.88, 142.19, 133.28, 133.19, 131.41, 131.21, 128.04, 128.00, 127.93, 126.15, 126.09, 126.05, 126.00, 125.83, 125.76, 125.72, 124.89, 124.84, 114.22, 113.99, 113.17, 113.13, 112.74, 112.71, 111.15, 111.08, 111.03, 104.80, 104.51, 104.46, 84.64, 83.18, 83.12, 83.05, 82.97, 81.95, 81.89, 81.58, 81.54, 75.03, 70.93, 70.70, 70.15, 69.92, 60.45, 60.12, 56.18, 56.17, 55.93, 55.92, 53.09, 53.08, 53.07, 53.05, 44.97, 43.65, 41.21, 41.13, 41.04, 40.96, 22.46, 22.39, 22.37, 22.35, 22.29, 22.25, 18.24, 18.14, 18.03, 17.93, 17.12, 17.09. ^{31}P-NMR (202 MHz, $CDCl_3$): 148.59, 148.10. HR-LSI-MS: 770.33093 ($[M+H]^+$, $C_{41}H_{49}N_5O_8P^+$; calc. 770.331878).

*[1,2,4]Triazolo[1,5-*c*]pyrimidin-5(1*H*)-one* (**12**). To a soln. of **11** (530 mg, 3.25 mmol; prepared as described [19]) in dry DMF (80 ml), $HC(OEt)_3$ (16.6 ml, 0.1 mmol) and conc. HCl (1.6 ml) were added. The mixture was heated overnight to 130°. After evaporation of solvents and purification by CC (SiO_2, AcOEt/MeOH 10:1), **2** (442 mg, 100%) was obtained. White solid. M.p. >200°. ^{1}H-NMR (300 MHz, (D_6)DMSO): 12.09 (br. *s*, 1 H); 8.41 (*s*, 1 H); 7.57 (*d*, *J* = 5.88, 1 H); 6.76 (*d*, *J* = 5.88, 1 H). ^{13}C-NMR (300 MHz, (D_6)DMSO): 154.31, 145.50, 134.87, 95.86. EI-MS: 136 (38, M^+), 108 (32), 95 (16), 81 (20).

*6-(3′,5′-Di-*O*-acetyl-2′-deoxy-*D*-ribofuranosyl)[1,2,4]triazolo[1,5-*c*]pyrimidin-5(6*H*)-one* (**13**). To a susp. of **12** (305.4 mg, 2.24 mmol) in MeCN (30 ml), **4** (517 mg, 2.23 mmol) and BSA (1.2 ml, 4.93 mmol, 2.2 equiv.) were added. After 30 min at r.t., the soln. was cooled to 0°, and $SnCl_4$ (0.525 ml, 4.93 mmol, 2.2 equiv.) was added slowly. The mixture was allowed to warm to r.t., and, after 3.5 h, sat. NaCl soln. (75 ml) was added. The mixture was extracted with CH_2Cl_2 (2×), the combined org. layer dried ($MgSO_4$) and evaporated, and the residue purified by CC (SiO_2, AcOEt/MeOH 10:1): **13** (612 mg, 82%; α-D/β-D 1:1). Colorless oil. ^{1}H-NMR (300 MHz, (D_6)DMSO): 8.27 (*s*, 1 H); 7.57, 7.63 (2*d*, *J* = 8.07, 1 H); 6.73 (*t*, *J* = 7.17, 1 H); 6.51 (*t*, *J* = 5.52, 0.5 H); 6.46 (*d*, *J* = 5.88, 0.5 H); 5.25 (*d*, *J* = 5.88, 1 H); 4.39–4.68 (*m*, 1 H); 4.23–4.37 (*m*, 2 H); 2.19–2.96 (*m*, 2 H). ^{13}C-NMR (300 MHz, (D_6)DMSO): 169.58, 154.69, 152.89, 144.41, 130.99, 97.10, 95.79, 88.63, 86.48, 85.14, 82.70, 73.79, 63.35, 38.13, 20.50. HR-LSI-MS: 337.114750 ($[M+H]^+$; $C_{14}H_{17}N_4O_6^+$; calc. 337.114810).

X-Ray Analysis of α-D-**13**. A suitable crystal (0.50 × 0.30 × 0.15 mm) was obtained from the soln. of a chromatographically enriched α-D-fraction in CH_2Cl_2/hexane in the form of a colorless rod; monoclinic space group *P*2(1). Intensity data were collected at 223 K on a *Stoe Image Plate* diffraction system (Mo*Kα*, *λ* 0.71073 Å). Of The 2867 independent reflections (*θ* = 2.03–25–85°), 2618 with $F > 2\sigma(I)$ were used in the refinement. The structure was solved by direct methods with SHELXS-97 and refined with SHELXL-97. The non-H-atoms were refined anisotropically, by means of weighted full-matrix least-squares on F^2. H-Atoms were included in calculated positions and treated as riding atoms with SHELXL-97 default parameters (AFIX 137 for the methyl H-atoms). The refinement converged at *R* = 0.0264, *s* = 0.993.

*6-(2′-Deoxy-*D*-ribofuranosyl)[1,2,4]triazolo[1,5-*c*]pyrimidin-5(6*H*)-one* (14). A soln. of **13** (564 mg, 1.67 mmol) in MeOH/conc. NH_3 soln. 1:1 (180 ml) was allowed to warm up from −20° to r.t. overnight. After evaporation, the crude product was washed with CH_2Cl_2 to give **14** (205 mg, 48%). White solid. ^{1}H-NMR (300 MHz, (D_6)DMSO): 8.41 (*d*, *J* = 2.22, 1 H); 7.98 (*dd*, *J* = 7.71, 8.1, 1 H); 6.86 (*dd*, *J* = 5.52, 2.19, 1 H); 6.30–6.38 (*m*, 1 H); 5.26–5.30 (*m*, 1 H); 5.10 (*m*, 1 H); 4.88 (*t*, *J* = 4.59, 1 H); 3.87–4.28 (*m*, 1 H); 3.41–3.61 (*m*, 2 H); 2.04–2.93 (*m*, 2 H). ^{13}C-NMR (300 MHz, (D_6)DMSO): 181.63, 180.19, 171.63, 160.27, 122.34, 117.31, 113.09, 97.07, 88.00, 72.62. HR-LSI-MS: 253.094940 ($[M+H]^+$; $C_{10}H_{13}N_4O_4^+$; calc. 253.093680).

*6-(2′-Deoxy-5′-*O*-[(4,4′-dimethoxytriphenyl)methyl]-*D*-ribofuranosyl)[1,2,4]triazolo[1,5-*c*]pyrimidin-5(6*H*)-one* (**15**). As described for **7** and **8**; from **14** (400 mg, 1.58 mmol). CC (SiO_2, CH_2Cl_2/MeOH/Et_3N 97:2:1) gave both **15** and its α-D anomer separately.

α-D-Anomer of **15**: 166 mg (19%). ^{1}H-NMR (300 MHz, $CDCl_3$): 8.15 (*s*, 1 H); 7.83 (*d*, *J* = 7.71, 1 H); 7.41–6.80 (*m*, 13 H); 6.64 (*d*, *J* = 8.1, 1 H); 6.47 (*d*, *J* = 5.88, 1 H); 4.52 (*t*, *J* = 4.05, 1 H); 4.47 (*d*, *J* = 5.52, 1 H); 3.77 (*s*, 6 H); 3.31–3.15 (*m*, 2 H); 2.82 (*q*, *J* = 6.96, 1 H); 2.49 (*q*, *J* = 7.35, 1 H). ^{13}C-NMR (300 MHz, $CDCl_3$): 158.55, 154.54, 153.41, 144.84, 144.39, 135.48, 133.39, 129.94, 127.91, 126.93, 113.20, 95.75, 89.49, 89.28, 86.58, 72.33, 63.96, 55.19, 41.63. HR-LSI-MS: 555.224670 ($[M+1]^+$, $C_{31}H_{31}N_4O_6^+$; calc. 555.224360).

β-D-Anomer **15**: 210 mg (24%). ^{1}H-NMR (300 MHz, $CDCl_3$): 8.16 (*s*, 1 H); 8.00 (*d*, *J* = 7.71, 1 H); 7.37–6.77 (*m*, 13 H); 6.52 (*t*, *J* = 6.24, 1 H); 6.27 (*d*, *J* = 8.07, 1 H); 4.65 (*t*, *J* = 4.95, 1 H); 4.08 (*m*, 1 H); 3.73 (*s*, 6 H); 3.43 (*m*, 2 H); 2.56 (*m*, 1 H); 2.29 (*m*, 1 H). ^{13}C-NMR (300 MHz, $CDCl_3$): 158.68, 154.77, 153.20, 144.77, 144.20,

135.08, 132.55, 129.90, 127.89, 127.18, 113.26, 96.66, 87.13, 86.46, 86.37, 71.02, 62.58, 55.23, 41.80. FAB-MS (pos.): 631 (85, $[M+76]^+$), 555 (23, $[M+1]^+$), 303 (100).

*6-[2′-Deoxy-5′-*O*-[(4,4′-dimethoxytriphenyl)methyl]-β-*D*-ribofuranosyl][1,2,4]triazolo[1,5-*c*]pyrimidin-5(6*H*)-one 3′-(2-Cyanoethyl Diisopropylphosphoramidite)* (**16**). As described for **9**, from **15** (β-D-anomer; 72 mg, 0.13 mmol). CC (SiO_2, AcOEt/hexane 1:1 (1% Et_3N) gave **16** (71 mg, 72.4%). White foam. ^{1}H-NMR (300 MHz, $CDCl_3$): 8.22 (*s*, 1 H); 7.99 (*dd*, *J* = 18, 8.1, 1 H); 7.40–6.80 (*m*, 13 H); 6.25 (*dd*, *J* = 7.71, 2.94, 1 H); 6.53 (*dd*, *J* = 10.68, 5.88, 1 H); 4.72 (*m*, 1 H); 4.17 (*dd*, *J* = 11.76, 2.94, 1 H); 3.77 (*s*, 6 H); 3.63–3.35 (*m*, 5 H); 2.71–2.59 (*m*, 2 H); 2.46–2.42 (*m*, 2 H); 1.25–1.06 (*m*, 12 H). ^{13}C-NMR (300 MHz, $CDCl_3$): 158.67, 154.75, 153.19, 144.71, 144.12, 134.97, 132.42, 130.09, 127.94, 127.11, 117.32, 112.97, 96.69, 87.00, 86.28, 85.62, 71.86, 62.06, 57.96, 55.19, 43.09, 40.80, 24.41, 20.12. ^{31}P-NMR (300 MHz, $CDCl_3$): 149.2, 148.7. HR-LSI-MS: 755.341310 ($[M+H]^+$, $C_{40}H_{48}N_6O_7P^+$; calc. 755.332212).

Oligonucleotide Synthesis. Oligonucleotides (*Table 5*) were synthesized with a *Pharmacia Gene-Assembler-Special* DNA synthesizer using standard 2-cyanoethyl phosphoramidite chemistry. Reagents and concentrations were as for the synthesis of natural DNA oligomers. The nonstandard phosphoramidite building blocks ^{8Br}G, ^{F}C, and C (*Fig. 3*) were from *Glen Research*. Syntheses were performed on a 1.3-μmol scale, according to the manufacturer's protocol. The only change made in the usual synthesis cycle was the prolongation of the coupling time for the nonstandard building blocks to 6 min. Coupling yields were typically higher than 98% also for non-standard phosphoramidites. After chain assembly and final detritylation, the oligomers were removed from the support and deprotected by treatment with *ca.* 2 ml of conc. NH_3 soln. (55°, 16 h). The crude oligonucleotides were purified by ion-exchange HPLC (*MonoQ HR 10/10* (*Pharmacia*) column). The isolated oligonucleotides were desalted over *SEP-PAK-C-18* cartridges (*Waters*) according to standard procedures. The oligonucleotides were further characterized by MALDI-TOF- or ESI-MS. *Table 5* shows MS data of the oligonucleotides containing nonstandard nucleotide units.

Table 5. *Calculated and Experimental Masses (*M^+*) of Oligonucleotides from ESI-MS*

Deoxyoligonucleotide	*m/z*	
	found	calc.
5′-d(TTTTTCT$^{4\,H}$TTCTCTCT)-3′	4480	4476[a])
5′-d(TTTTTCT$^{\alpha}$QTCTCTCT)-3′	4504	4505
5′-d(TTTTTCT$^{\beta}$QTCTCTCT)-3′	4504	4505
5′-d(GCTAAAAAGA^{F}CAGAGAGATCG)-3′	6539	6538
5′-d(TTTTTTT$^{\beta}$Q TTTTTTT)-3′	4509	4509
5′-d(GCTAAAAAGA^{8Br}GAGAGAGATCG)-3′	6640	6639

[a]) Data from MALDI-TOF-MS.

UV/Melting Experiments. Melting experiments were performed on a *Cary-3E-UV/VIS* spectrophotometer (*Varian*). Melting curves (λ 260 nm) were recorded for a consecutive heating($0 \rightarrow 90°$)-cooling-heating protocol with a linear gradient of 0.5°/min. All measurements were performed in buffered solns. (10 mM Na-cacodylate, 100 mM NaCl, 0.25 mM spermine). Stoichiometric amounts of each strand were used for triplex formation, and the triplex conc. was kept at 1.7–2.0 μM. The final pH was adjusted to the desired values with 0.1M HCl or 0.1M NaOH. T_m Data were obtained from the first derivative of the heating cycle. As in almost all cases, hysteresis formation was observed for third-strand melting and annealing; these data do not reflect equilibrium binding conditions.

REFERENCES

[1] S. Neidle, *Anti-Cancer Drug Design* **1997**, *12*, 433.
[2] D. Praseuth, A. L. Guieysse, C. Hélène, *Biochim. Biophys. Acta* **1999**, *1489*, 181.
[3] H. E. Moser, P. B. Dervan, *Science (Washington, D.C.)* **1987**, *238*, 645.
[4] J.-C. François, T. Saison-Behmoaras, C. Hélène, *Nucleic Acids Res.* **1988**, *16*, 11431.
[5] P. A. Beal, P. B. Dervan, *Science (Washington, D.C.)* **1991**, *251*, 1360.

[6] R. H. Durland, D. J. Kessler, S. Gunnell, M. Duvic, B. M. Pettitt, M. E. Hogan, *Biochemistry* **1991**, *30*, 9246.
[7] K. R. Fox, *Curr. Med. Chem.* **2000**, *7*, 17.
[8] H.-U. Stilz, P. B. Dervan, *Biochemistry* **1993**, *32*, 2177.
[9] D. M. Gowers, J. Bijapur, T. Brown, K. R. Fox, *Biochemistry* **1999**, *38*, 13747.
[10] T. E. Lehmann, W. A. Greenberg, D. A. Liberles, C. K. Wada, P. B. Dervan, *Helv. Chim. Acta* **1997**, *80*, 2002.
[11] C.-Y. Huang, G. Bi, P. S. Miller, *Nucleic Acids Res.* **1996**, *24*, 2606.
[12] R. H. Durland, T. S. Rao, V. Bodepudi, D. M. Seth, K. Jayaraman, G. R. Revankar, *Nucleic Acids Res.* **1995**, *23*, 647.
[13] J. Marfurt, S. P. Parel, C. J. Leumann, *Nucleic Acids Res.* **1997**, *25*, 1875.
[14] J. Marfurt, C. Leumann, *Angew. Chem.* **1998**, *110*, 184; *Angew. Chem., Int. Ed.* **1998**, *37*, 175.
[15] I. Prévot-Halter, C. Leumann, *Bioorg. Med. Chem. Lett.* **1999**, *9*, 2657.
[16] J. P. Dirlam, R. B. James, E. V. Shoop, *J. Heterocycl. Chem.* **1980**, *17*, 409.
[17] J. Bradac, Z. Furek, D. Janezic, S. Molan, I. Smerkolj, B. Stanovnik, M. Tisler, B. Vercek, *J. Org. Chem.* **1977**, *42*, 4197.
[18] H. Vorbrüggen, B. Bennua, *Chem. Ber.* **1981**, *114*, 1279.
[19] V. Nair, A. G. Lyons, D. F. Purdy, *Tetrahedron* **1991**, *47*, 8949.
[20] K. Kohda, I. Kobayashi, K. Itano, S. Asano, Y. Kawazoe, *Tetrahedron* **1993**, *49*, 3947.
[21] 'Oligonucleotides and Analogues – A Practical Approach', Ed. F. Eckstein, Oxford University Press, Oxford, 1991.
[22] W. Saenger, 'Principles of Nucleic Acid Structure', Springer-Verlag, New York, 1984.
[23] T. Brown, G. A. Leonard, E. D. Booth, J. Chambers, *J. Mol. Biol.* **1989**, *207*, 455.
[24] N. Peyret, P. A. Seneviratne, H. T. Allawi, J. SantaLucia Jr., *Biochemistry* **1999**, *38*, 3468.
[25] A. A. Koshkin, S. K. Singh, P. Nielsen, V. K. Rajwanshi, R. Kumar, M. Meldgaard, C. E. Olsen, J. Wengel, *Tetrahedron* **1998**, *54*, 3607.
[26] S. Obika, D. Nanbu, Y. Hari, J.-I. Andoh, K.-I. Morio, T. Doi, T. Imanishi, *Tetrahedron Lett.* **1998**, *39*, 5401.
[27] M. J. J. Blommers, F. Natt, W. Jahnke, B. Cuenoud, *Biochemistry* **1998**, *37*, 17714.
[28] B. Cuenoud, F. Casset, D. Hüsken, F. Natt, R. M. Wolf, K.-H. Altmann, P. Martin, H. E. Moser, *Angew. Chem.* **1998**, *110*, 1350; *Angew. Chem., Int. Ed.* **1998**, *37*, 1288.
[29] S. Obika, Y. Hari, M. Sekiguchi, T. Imanishi, *Angew. Chem.* **2001**, *113*, 2149; *Angew. Chem., Int. Ed.* **2001**, *40*, 2079.

Received August 23, 2001